Atmospheric Environment 209 (2019) 14–22

Contents lists available at ScienceDirect

Atmospheric Environment

journal homepage: www.elsevier.com/locate/atmosenv

MODIS AOD sampling rate and its effect on $PM_{2.5}$ estimation in North China

Zijue Song[a,b], Disong Fu[a,d], Xiaoling Zhang[b], Xinlei Han[a,d], Jingjing Song[a,d], Jinqiang Zhang[a], Jun Wang[e], Xiangao Xia[a,c,d,*]

[a] LAGEO, Institute of Atmospheric Physics, Chinese Academy of Sciences, Beijing, 100029, China
[b] Chengdu University of Information Technology, Chengdu, 610225, China
[c] Collaborative Innovation Center on Forecast and Evaluation of Meteorological Disasters, Nanjing University of Information Science & Technology, Nanjing, 210044, China
[d] College of Earth and Planetary Sciences, University of Chinese Academy of Sciences, Beijing, 100049, China
[e] Department of Chemical and Biochemical Engineering, Center for Global and Regional Environmental Studies, and Informatics Initiative, The University of Iowa, Iowa City, IA, 52241, USA

ARTICLE INFO

Keywords:
Aerosol optical depth
$PM_{2.5}$
Sampling rate
Data filling

ABSTRACT

Much attention has been paid to develop methods to estimate particulate matter with an aerodynamic diameter of 2.5 μm or less ($PM_{2.5}$) from satellite aerosol optical depth (AOD). One of fundamental limitation of these methods is lack of AOD and thereby $PM_{2.5}$ cannot be derived from satellites when clouds are present or when surface conditions are not favorable. This would probably result in an inherent clear-sky biased estimate of $PM_{2.5}$ for air quality assessment that requires continuous 24-h measurements at all-sky conditions. Using the Moderate Resolution Imaging Spectroradiometer (MODIS) AOD and $PM_{2.5}$ data in North China, a highly polluted area with large spatiotemporal variabilities of AOD and $PM_{2.5}$ values, missing MODIS AOD retrievals and its potential effect on $PM_{2.5}$ estimation are studied. The MODIS dark target (DT) algorithm produces very few AODs in winter, with a regional observation rate of 4%, which limits its statistical significance for $PM_{2.5}$ air quality monitoring. This limitation applies to MODIS DT AOD products at 10-km and 3-km resolutions since they are derived from the same retrieval core (Remer et al., 2013). In contrast, The MODIS deep blue (DB) AOD product complements the MODIS DT AOD coverage, which is remarkable in winter. The MODIS DT and DB merged product has comparable accuracy to that of the DT and DB products but shows a larger sampling rate, therefore, it is more suitable for estimating surface $PM_{2.5}$. While the regional mean $PM_{2.5}$ values in the presence and absence of AOD retrievals in spring and summer are comparable, but the former is substantially lower than the latter in autumn by 11.2 $\mu g m^{-3}$ and winter by 8.5 $\mu g m^{-3}$ on average. The difference in some stations even exceeds 20 $\mu g m^{-3}$. Methods to fill missing AOD values in North China are crucial to provide an unbiased sampling and estimate of $PM_{2.5}$ concentration in all-sky conditions, likely by integrating satellite, surface and modeling data.

1. Introduction

Ambient fine particulate matter with aerodynamic diameter of < 2.5 μm ($PM_{2.5}$) shows the most consistent association with adverse health outcomes and therefore is one of significant public health concern (Pope and Dockery, 2006; Kloog et al., 2013; WHO, 2016). $PM_{2.5}$ is affecting more people worldwide than any other pollutants, especially in developing world, for example, over 1.3 billion people suffer from $PM_{2.5}$ health risks in China (Cohen et al., 2017; Song et al., 2017). Significant short-term positive associations of mortality with $PM_{2.5}$ in Xi'an and Beijing, two heavily polluted cities, were revealed (Cao et al., 2012; Li et al., 2013). Obtaining accurate local $PM_{2.5}$ concentrations plays a central role in addressing this public health concern. Typically, exposure to $PM_{2.5}$ in such epidemiological studies is assessed using surface level $PM_{2.5}$ measurements. These measurements often lack adequate spatial resolution to capture variability in the study population exposure, although regional $PM_{2.5}$ monitoring networks have been established (Pui et al., 2014). Because satellite remote sensing has the capacity to provide data with large spatial coverage, it holds promise for adding spatial information for $PM_{2.5}$ distribution and exposure studies, particularly in suburban and rural areas far from monitors (Engel-Cox et al., 2004).

Satellite retrieved aerosol optical depth (AOD: the column-integrated extinction) is a good surrogate for $PM_{2.5}$, while these two parameters are not expected to be strictly correlated because the former represents ambient column-integrated aerosol extinction and the latter

* Corresponding author. #40, Huayanli, Chaoyang District, Beijing, 100029, LAGEO, Institute of Atmospheric Physics, Chinese Academy of Sciences, China.
E-mail address: xxa@mail.iap.ac.cn (X. Xia).

https://doi.org/10.1016/j.atmosenv.2019.04.020
Received 25 October 2018; Received in revised form 6 April 2019; Accepted 8 April 2019
Available online 13 April 2019
1352-2310/

represents dry particulate matter mass near surface (Hoff and Christopher, 2009; Chudnovsky et al., 2013a,b). Satellite-based $PM_{2.5}$ estimation methods have been developed, varying from calibrating AODs with only $PM_{2.5}$ at ground monitoring stations (Lü et al., 2016) to a hybrid approach incorporating AOD, land use and meteorological variables to estimate $PM_{2.5}$ (KloogKoutrakis et al., 2011; Chudnovsky et al., 2013a,b; Liang et al., 2018; Zhang et al., 2018). Long-term exposure assessment in North Carolina based on satellite-based $PM_{2.5}$ estimations showed equivalent outcome to that of central site monitored data (McGuinn et al., 2018). One of causes for this unexpected result was likely associated with potential $PM_{2.5}$ estimation errors. Note that satellite derived $PM_{2.5}$ is highly dependent on the amount of AOD retrievals. AOD is required not only for the development of AOD-$PM_{2.5}$ relationship since it shows large spatiotemporal variabilities, but also for its application (Chudnovsky et al., 2013a; b). AOD is only probably retrieved under cloudless sky conditions. As a matter of fact, snow cover or misclassification of a heavy aerosol layer into clouds can result in AOD unavailable even under clear-sky conditions. Satellite AOD sampling rate shows a large spatiotemporal variabilities that highly depends on climate and surface condition (Chudnovsky et al., 2013b; Liang et al., 2018; Zhang et al., 2018; Lee et al., 2018). Therefore, potential differences in $PM_{2.5}$ values between two contrasting conditions, i.e., in the presence and absence of AOD retrievals, should be carefully evaluated, which has important implications for satellite studies especially over areas where ground-based measurements are rare and spatiotemporal variation of $PM_{2.5}$ is large (Gupta and Christopher, 2008). This is exactly why we select North China (NC: 34.4–42.6° N; 113.5–122.7° E), the heavily polluted region in China, as our research object in this paper.

Moderate Resolution Imaging Spectroradiometer (MODIS) AOD is one of widely used satellite products in the air quality study. In this paper, the quality and sample rates of latest MODIS AOD products are firstly analyzed. Potential bias of $PM_{2.5}$ prediction due to missing AODs is then quantitatively evaluated, which is achieved by comparing surface-level $PM_{2.5}$ concentrations in the presence of AOD with that in the absence of AOD. The paper is organized as follows. Section 2 introduces MODIS AOD and surface $PM_{2.5}$ data. Comparison of MODIS three data products is presented in section 3. The difference between $PM_{2.5}$ mass in the presence of MODIS AOD and no AOD retrieval ($\Delta PM_{2.5}$) is finally analyzed. Implication of this difference in the estimation of $PM_{2.5}$ from space in NC is discussed.

2. Study region, data and methodology

2.1. Study region

NC is surrounded by Yan Mountain to the north and by Taihang Mountain to the west. NC faces Bohai Bay and Yellow Sea to the east (Fig. 1). Due to its specific terrain and huge amount of anthropogenic emissions of primary aerosols and production of secondary aerosols, NC suffers frequent pollution events, especially in the winter (Fu et al., 2018).

2.2. Ground-level $PM_{2.5}$ mass

Hourly $PM_{2.5}$ concentrations from May 2014 to May 2018 at 159 monitors (Fig. 1) are available from the website of the China Environmental Monitoring Center (CEMC) (http://106.37.208.233:20035/). $PM_{2.5}$ concentrations are routinely monitored by the TEOM and/or BAM according to the environmental protection standard of China. Calibration of instruments and data quality control are conducted by CEMC. A smooth temporal variability filter was further used to eliminate records of consecutive invariant $PM_{2.5}$ mass, i.e., five consecutive hourly $PM_{2.5}$ measurements with the same value were excluded. Furthermore, a spike filter was used to eliminate records that constituted a large spike (positive or negative) during a short period of time. A spike is defined when $PM_{2.5}$ in the middle of 5 consecutive records is three times higher than the standard deviation (calculated from remaining 4 records before and after data points that is being examined).

2.3. AERONET AOD

Sunphotometer AOD in Beijing (BJ: 39.977° N, 116.381° E, 92 m a.s.l.) and Xianghe (XH: 39.754° N, 116.962° E, 36 m a.s.l.) during 2002–2017 are used to validate MODIS AOD. Both are Aerosol Robotic Network (AERONET) stations, but characterized by distinctly different land surface, i.e., urban surface in BJ and a mixture of agricultural land and settlement place in XH. Spectral AOD with accuracy of 0.01–0.02 are derived from CE-318 sunphotometer measurements (Eck et al., 1999). AOD at 0.55 μm is interpolated from AOD at 0.44, 0.67 and 0.87 μm to compare with MODIS AOD product. The latest Version 3 cloud-screened and quality assured AOD data (Level 2.0) are used. The update of Version 3 is that only three channels (0.67, 0.87 and 1.02 μm) are checked for triplet variance. AODs are screened when the triplet range for all three wavelengths exceeds 0.01 or 0.015 × AOD (whatever is greater), which allows for unprecedented ability to monitor extreme fine mode pollution events (Eck et al., 2018; Song et al., 2018).

2.4. MODIS AOD

The Dark Target (DT) and Deep Blue (DB) algorithms are used for the retrievals of AOD. The DT works only over vegetated land (Kaufman et al., 1997). The DB method expands MODIS AOD coverage to bright surfaces by using MODIS reflectance measurement at 0.412 μm. Various refinements to the MODIS AOD retrieval algorithms have been made since the launch of MODIS, including updates in calibration, surface reflectance models, aerosol microphysical models, and cloud screening procedures (Levy et al., 2013; Hsu et al., 2013). The most recent full AOD reprocessing is C6 and C6.1. In addition to separate DT and DB retrievals, a merged AOD that combined both types of retrievals is provided that increases the spatial coverage of AOD over land while preserving its quality. The DT team also released a nominal 3-km product for the air quality study (Remer et al., 2013). An important update of C6.1 AOD data is a revised surface characterization over urban areas (Gupta et al., 2016). Furthermore, internal smoke detection masks are updated to identify thick and/or spatial variable smoke events (Eck et al., 2018). These improvements are of significance in NC since it is characterized by urban surface and frequent smoke layer in the harvest season (Xia et al., 2013; Zha et al., 2013).

2.5. Methods

A dramatic day-to-day variation is frequently observed in NC. A typical example is shown in Fig. 2, in which daily AERONET and MODIS 10-km AOD as well as $PM_{2.5}$ in Beijing during October 2015 in presented. Two aerosol pollution episodes were featured by an increase of one order of magnitude of AOD and $PM_{2.5}$ within a couple of days, and then both quantities suddenly dropped to the background level due to a frontal passage. Aqua-MODIS C6 and C6.1 Level 2.0 DT, DB and merged AOD products with a 10-km resolution are used in this study. The daily data are gridded into 0.1° by 0.1° using the nearest-neighbor interpolation method. MODIS AOD products are firstly validated against AERONET data to show potential improvements of MODIS C6.1 AOD relative to C6. In order to show spatiotemporal variations of AOD, coefficient of variations (COV) of AOD, i.e., the ratio of the standard deviation of AOD to the mean, at each grid are calculated in four seasons (MAM: March, April, and May; JJA: June, July and August; SON: September, October, November; DJF: December, January and February). Station $PM_{2.5}$ is collocated with the nearest MODIS AOD grid. $PM_{2.5}$ values are averaged if two or more stations are within one grid. The largest number of sites that fall on a single grid is 3 stations. Note that the representative area of $PM_{2.5}$ measurements at 1–3 stations

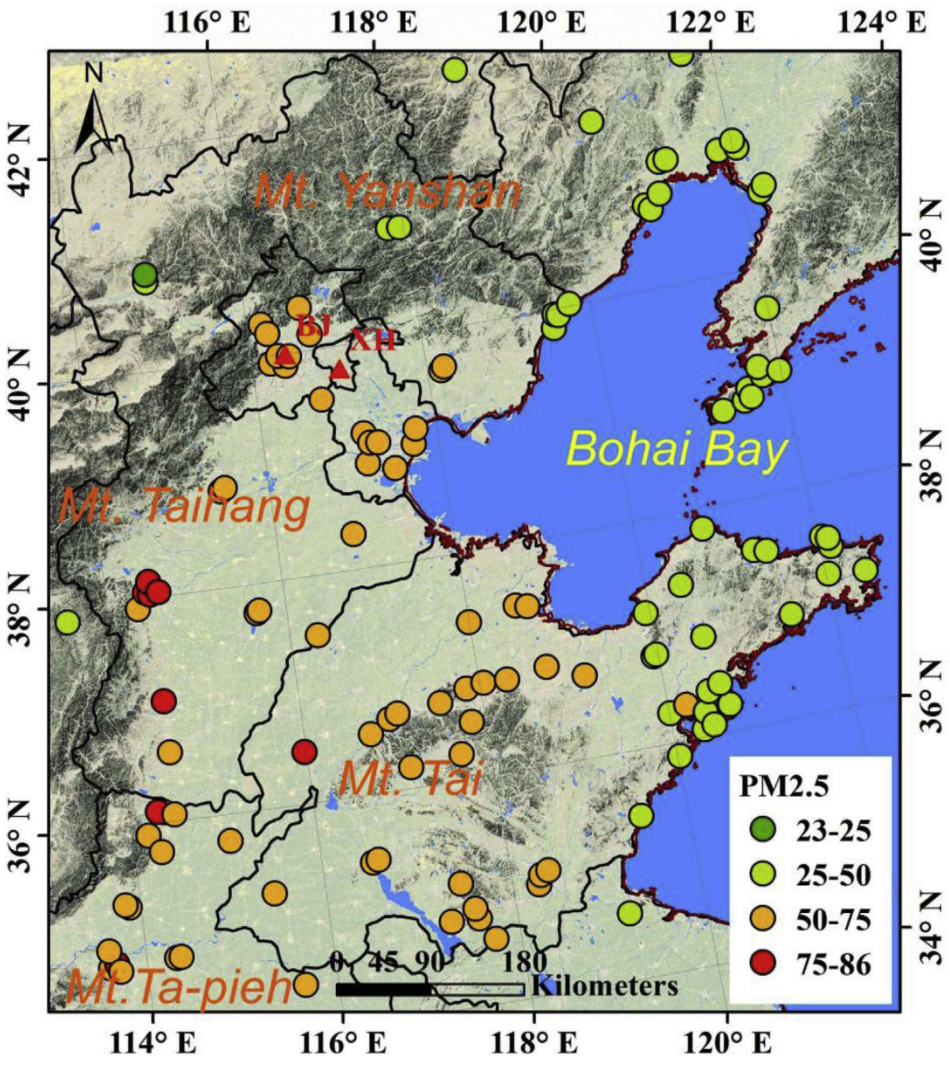

Fig. 1. Spatial distribution $PM_{2.5}$ stations and their annual average $PM_{2.5}$ concentration (μg m^{-3}) in North China.

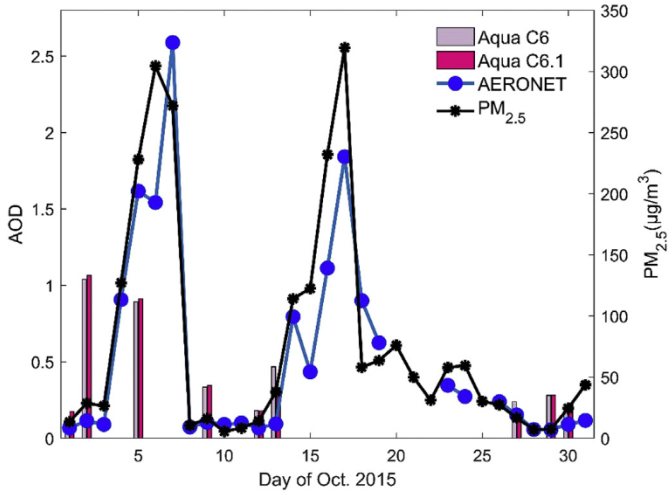

Fig. 2. Daily mean PM2.5 (μg m^{-3}) and AERONET AOD as well MODIS C6 and C6.1 AOD in Beijing during October of 2015.

depends on spatial variation of their local emission sources, which may not consist with the spatial representation of AOD (Shi et al., 2017). For grids with ground station available, seasonal mean $PM_{2.5}$ values are calculated separately under two contrast conditions, i.e., with and without AOD, respectively. Seasonal $\Delta PM_{2.5}$ values at 128 grids with $PM_{2.5}$ stations are calculated to answer the questions raised in this study.

3. Results and discussion

3.1. MODIS C6 and C6.1 AOD assessment result

Fig. 3 shows the comparison of MODIS DT, DB, merged AOD products against AREONET AOD in BJ (right panel) and XH (left panel), respectively. A few features merit mention. First, DT AOD bias was notably reduced in BJ, from 0.2 of C6 to 0.1 of C6.1, which met the expectation since a new surface reflectance scheme was introduced in urban regions (Gupta et al., 2016). C6.1 DT AOD products in XH showed little improvement. Second, C6 and C6.1 DB AOD products showed similar accuracy and C6.1 DB sampling points increased slightly relative to C6 DB. Third, the sampling rates of DB product were about twice larger than that of DT in BJ and 1.5 times larger in XH, respectively. This agreed with result of Tao et al. (2015) showing that C6 DB generally reveals spatial extent of the widespread haze pollution in NC in cases where there were few DT AODs. Fourth, notable improvement in the accuracy of C6.1 merged product relative to C6 was only found in BJ as a result of C.61 DT AOD improvement. Finally, the accuracy of merged AOD was comparable to that of DT and DB, but the sampling rate of merged AOD was larger.

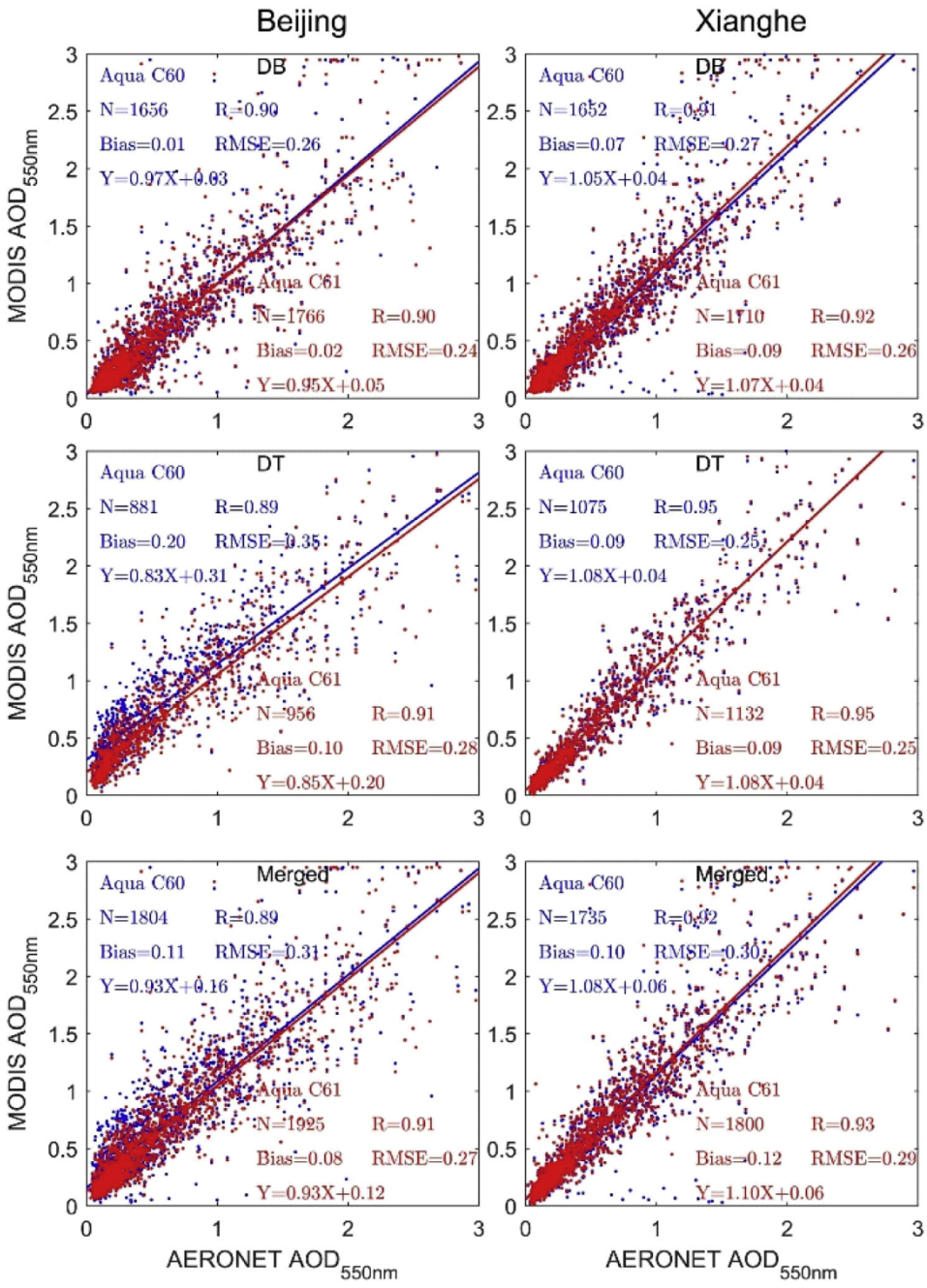

Fig. 3. Scatter-plot of collocated AERONET AOD and MODIS AOD product in Beijing (right) and Xianghe (left). Three MODIS AOD products were compared to AERONET ground truth, i.e., deep blue (DB: upper), dark target (DT: middle) and merged AOD product (bottom). (For interpretation of the references to colour in this figure legend, the reader is referred to the Web version of this article.)

DT AOD has been widely used before the release of C6. Actually, it is still a conventional product in the air quality study partly because of its 3-km product. The result showed that the DT AOD product had the lowest sampling rate among three products, especially in winter when a robust AOD-$PM_{2.5}$ relationship cannot be established from very few AOD-$PM_{2.5}$ pairs. One may argue that AOD-$PM_{2.5}$ relationships in other seasons can be used; this method, however, might very likely produce a large biased $PM_{2.5}$. This is because the AOD-$PM_{2.5}$ relationship highly depends on the boundary layer height that varies seasonally and leads to a contrast in the seasonality of AOD and $PM_{2.5}$ over NC (Xia et al., 2006). Distinct seasonal variations of AOD-$PM_{2.5}$ relationship can be easily evidenced by a simple AOD-$PM_{2.5}$ correlation analysis within different time scales. Fig. 4 shows R^2 and the slopes of the linear regression analysis of AERONET AOD and $PM_{2.5}$ in four seasons in BJ, which is compared with that based on all year round of AOD-$PM_{2.5}$ pairs. AOD showed a close relationship to $PM_{2.5}$ but it varies daily (Chudnovsky et al., 2012). R^2 ranges from 0.65 in spring to 0.73 in summer, which are all larger than R^2 (0.60) derived from all pairs of AOD and $PM_{2.5}$. AOD-$PM_{2.5}$ relationships differ substantially between seasons. The slopes are 95 in spring, 58 in summer, 118 in autumn, and 148 $\mu g\, m^{-3}$ per unit of AOD in winter, respectively. Obviously, lack of MODIS AOD in winter could not be remedied by borrowing AODs in other seasons. DT 3-km AOD product also suffers from a very low sampling rate in winter because it does not merge the DB algorithm. This would certainly produce a biased $PM_{2.5}$ especially in winter when very few DT 3-km AODs are used (Ma et al., 2014; Lü et al., 2016).

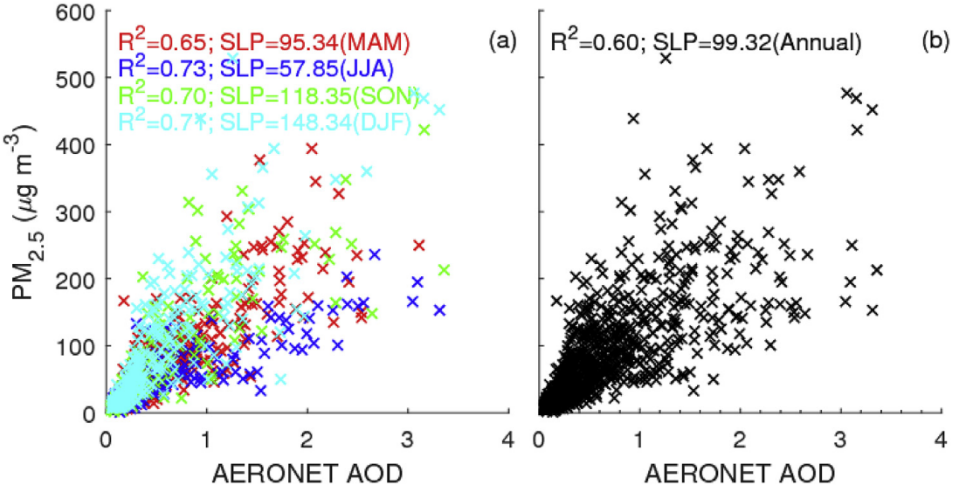

Fig. 4. R^2 and the slope of linear regression of PM2.5 to AERONET AOD in Beijing based on AOD-$PM_{2.5}$ pairs in spring (MAM), summer (JJA), autumn (SON) and winter (DJF) (a) and all year round of data pairs (b).

3.2. Spatial and temporal variability of MODIS AOD and AOD sampling rate

Spatial distribution of seasonal AOD coefficient of variations (COV) (the ratio of the standard deviation to the mean) is shown in Fig. 5. COVs show distinct spatial and seasonal dependences. Mountain COVs (in the north and the west of NC) exceeded 100%, which were somewhat larger than plain COVs (within 40–100%). This is partly because mountain AODs is much lower than plain AODs. In addition, this is also likely related to a relative lower AOD sampling rate over mountains (see below). The maximum and minimum seasonal COVs were observed in winter (a spatial average of 101%) and in summer (80%), which respectively corresponded to the maximum and minimum seasonal mean $PM_{2.5}$ value (Fu et al., 2018). In fall and winter, $PM_{2.5}$ and AOD often accumulate gradually as a result of stable weather, which is then followed by a dramatic drops due to a frontal passage (Fig. 2). This inevitably produces a substantial large AOD variation and then large COV.

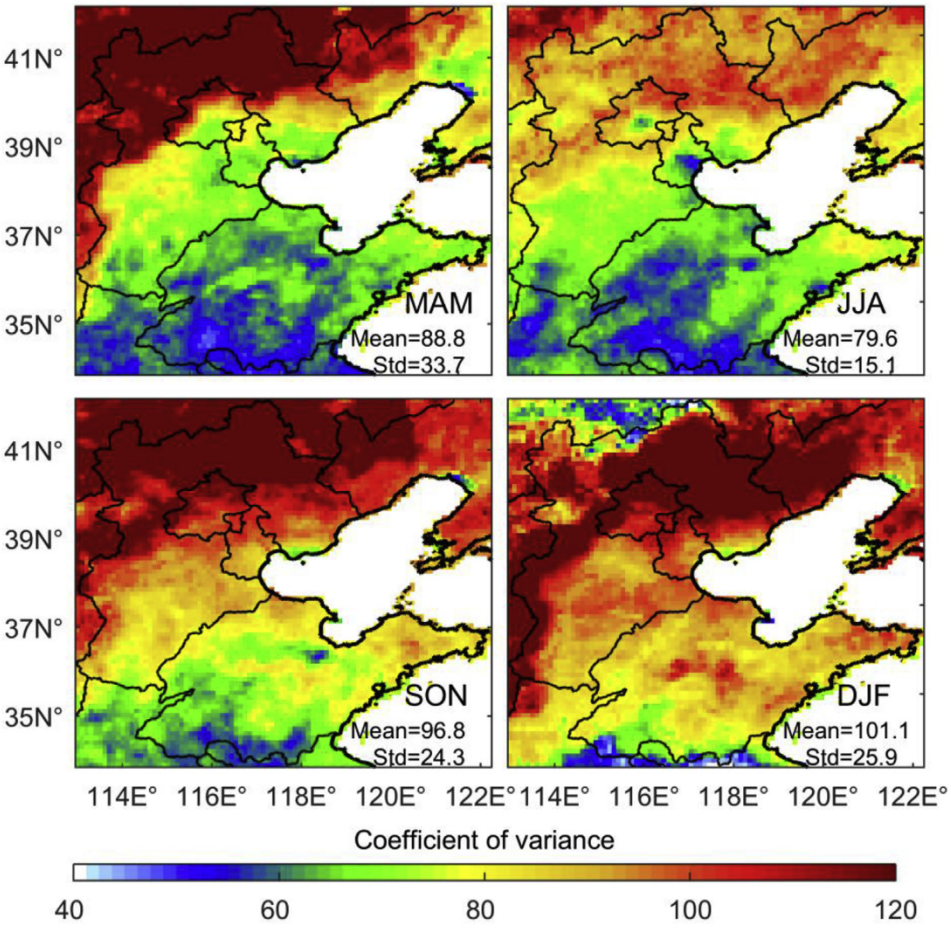

Fig. 5. Spatial distribution of seasonal coefficient of variation (COV) for AOD in North China. The regional mean and standard deviation of COV were also shown.

Table 1
The regional mean and standard deviation of the MODIS AOD sampling rates (the relative ratio of days with AOD retrieval to total days, unit: %) in North China. The calculations were performed on the basis of seasonal MODIS C6 and C6.1 three AOD products, i.e., dark target (DT), deep blue (DB) and merged (Merged) products, respectively.

	C6			C6.1		
	DT	DB	Merged	DT	DB	Merged
Spring	23.4 ± 14.1	37.9 ± 10.6	44.5 ± 8.2	23.2 ± 13.4	35.5 ± 11.4	42.6 ± 9.4
Summer	32.2 ± 6.6	17.6 ± 6.9	32.7 ± 5.9	31.7 ± 6.7	17.2 ± 6.3	32.1 ± 5.9
Autumn	33.4 ± 8.1	35.5 ± 11.4	43.2 ± 7.0	33.8 ± 8.0	36.0 ± 11.0	43.7 ± 7.0
Winter	3.6 ± 6.4	34.2 ± 14.9	36.4 ± 14.0	4.0 ± 6.9	34.8 ± 15.9	37.2 ± 14.5

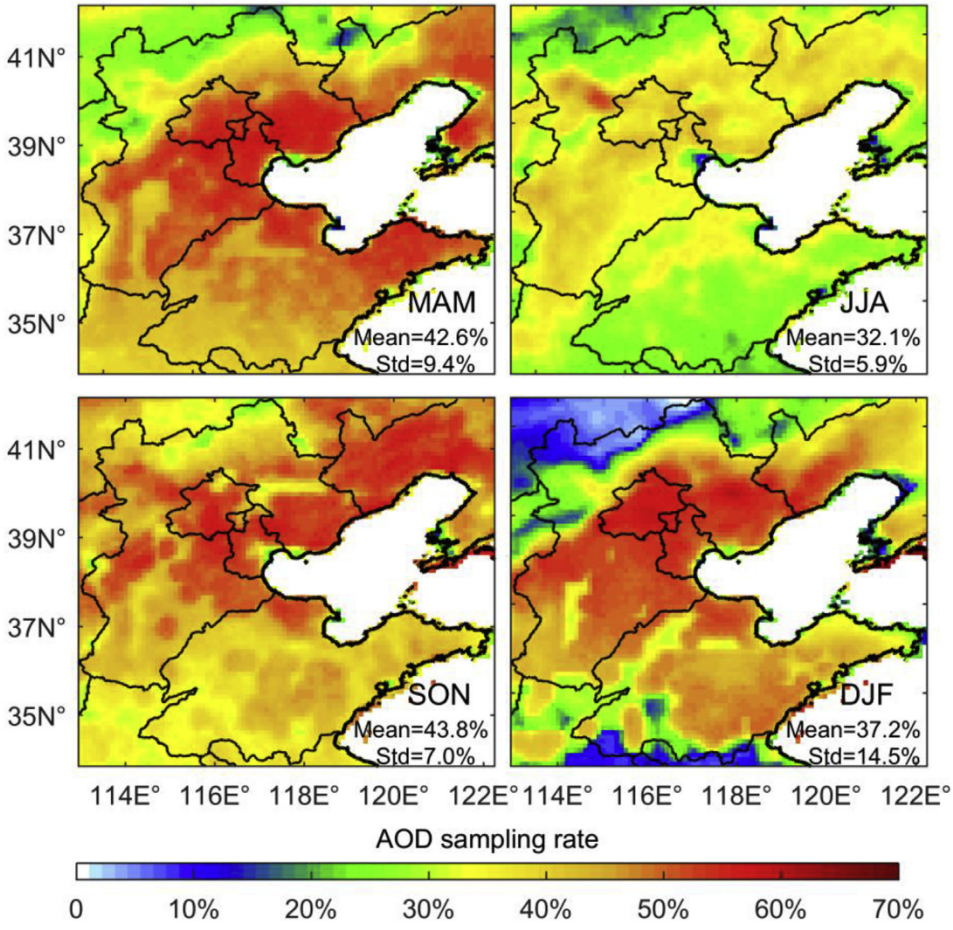

Fig. 6. Spatial distribution of the sampling rate of C6.1 merged AOD product (the relative ratio of days with AOD retrieval to total days, unit: %) in four seasons. The regional mean and standard deviation of sampling rate were also shown.

Table 1 presents the regional mean and standard deviation of MODIS AOD sampling rates that are calculated from C6 and C6.1 AOD products, i.e., DT, DB and merged in four seasons. Relative to C6 product, C6.1 AOD sampling rates increased marginally in autumn and winter, but they decreased slightly in spring and summer. The largest sampling rate was associated with the merged AOD product. This result was expected since the objective of this product was to increase the spatial coverage of AOD over land. The sampling rates of the DT AOD product were comparable to that of the DB product in spring, summer and fall, however, it was extremely low (about 4%) in winter. Seasonal gridded C6.1 merged AOD sampling rate is shown in Fig. 6. The sampling rate over mountains was relatively lower than that over plains. The sampling rate in the south of Hebei, Beijing and Tianjin was generally larger than that in Shandong peninsula by 10%. Summer is rainy season when the minimum sampling rate occurred, with a regional average of 32.1%. The merged AOD sampling rates in winter over plains were close to or even larger than that in autumn and spring. On the contrary, the DT AOD sampling rate in winter was strikingly low and it decreased from south to north (Fig. 7). This result also applies to the DT 3-km AOD product since the same retrieval core as that of the DT 10-km AOD product has been used. Additionally, another weakness of the DT 3-km product, despite its finer spatial resolution than the 10-km product, should not be overlooked, that is, the 3-km AOD over land compared less well with AERONET than did the 10-km AOD. Of particular interest for this study was that the 3-km product introduced a high-biased noise over bright and/or urban surfaces (Remer et al., 2013).

Merging DT and DB AOD products promoted the sampling rate remarkably relative to DT in spring (from 23.2% to 42.6%) and autumn (from 33.9% to 43.8%). However, there was only a marginal increase in summer (31.7% versus 32.1%). Except for the cloud mask, the DT algorithm does not work in cases when surface reflectance at visible-

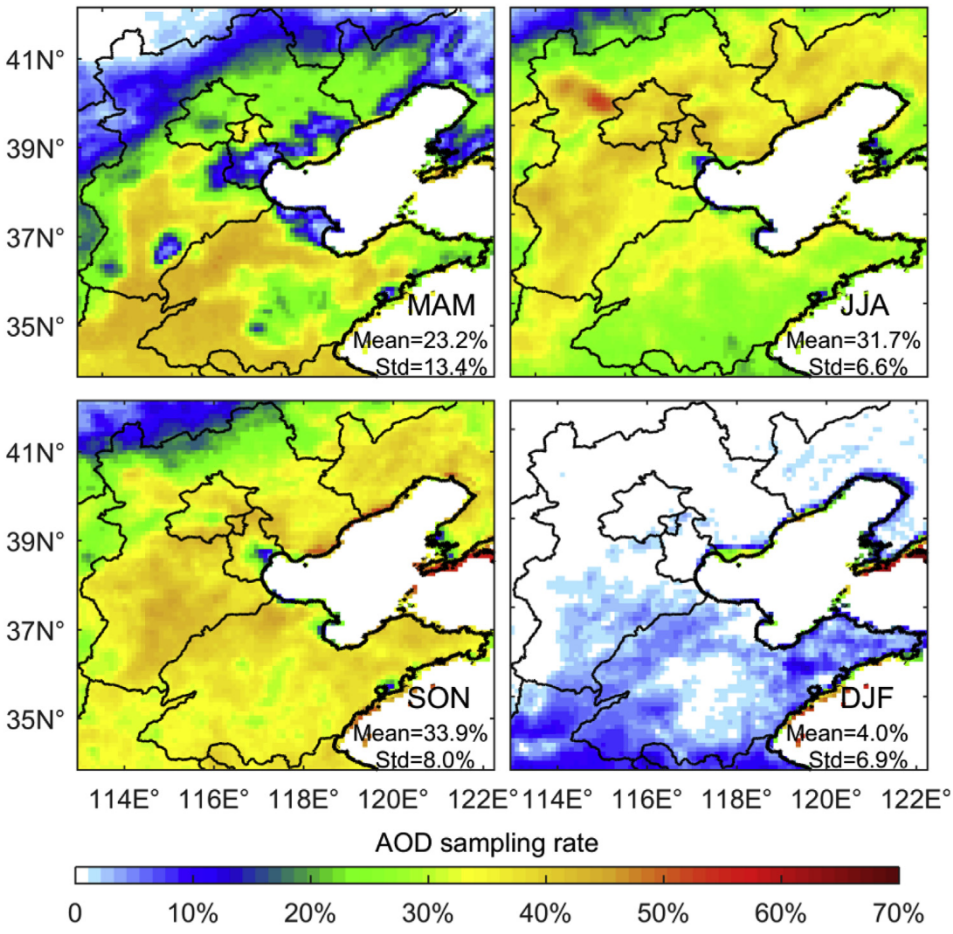

Fig. 7. Similar as Fig. 6 but for C6.1 DT AOD product.

infrared channels exceeds specified thresholds, which are not uncommon in early spring before the winter wheat turns green and in winter when crops wither. So, it is natural that the DB sampling rates in seasons except in summer are always larger than that of the DT. The DB sampling rate (17.2%) in summer was much less than that of DT (31.7%), which was likely because of its stringent cloud that more often erroneously removed cloud-free pixels (Hsu et al., 2013).

Fig. 8 presents seasonal $\Delta PM_{2.5}$ values at each grid with at least one $PM_{2.5}$ station. Note, to maximize the AOD availability, MODIS C6.1 merged AODs were used to calculate $\Delta PM_{2.5}$. Histogram of $PM_{2.5}$ associated with these two contrasting situations is also embedded. The squares and circles represent that $\Delta PM_{2.5}$ is lower/higher than zero, respectively. $\Delta PM_{2.5}$ values that are significantly different from zero at a confidence level of 95% are represented by the solid markers; on the contrary, the open markers mean not. In spring, most $\Delta PM_{2.5}$ values were within $\pm 5\,\mu g\,m^{-3}$ and the differences were not significant. The spatial mean $\Delta PM_{2.5}$ was $-1.3 \pm 6.5\,\mu g\,m^{-3}$. The $PM_{2.5}$ histograms under two contrasting situations were also similar. These facts indicated that missing AOD retrievals would not likely produce a significant biased $PM_{2.5}$, especially for the spatial mean $PM_{2.5}$ value. This was likely true in summer when the spatial mean $\Delta PM_{2.5}$ was $-1.7 \pm 6.4\,\mu g\,m^{-3}$. Large $\Delta PM_{2.5}$ values were observed in autumn and winter, with spatial mean $\Delta PM_{2.5}$ values being $-11.2 \pm 11.6\,\mu g\,m^{-3}$ and -8.5 $\pm$ 13.4 $\mu g\,m^{-3}$, respectively. Specifically, significantly negative $\Delta PM_{2.5}$ values were observed at stations located in South of Hebei Province, Beijing as well as North of Henan Province where $\Delta PM_{2.5}$ exceeded $-20\,\mu g\,m^{-3}$ (that reached 30% of the seasonal mean of $PM_{2.5}$). This feature was originated from a relatively lower frequency of smaller $PM_{2.5}$ values than $35\,\mu g\,m^{-3}$ and higher frequency of larger $PM_{2.5}$ values than $75\,\mu g\,m^{-3}$ in the absence of AOD relative to the presence of AOD.

Large temporal variability in AOD in East China indicated that long record lengths to achieve statistical stability (Lee et al., 2018). The fact that MODIS AOD products prevail over other satellite AOD products in the air quality study lies in their high quality and good spatiotemporal coverage, which is enhanced by merging DT and DB products. However, low MODIS AOD retrievals and dramatic temporal variation of $PM_{2.5}$ in NC need further consideration in estimating $PM_{2.5}$ from AOD. Multi-sensor AOD products from many polar-orbing sensors are likely complementary in accuracy and spatiotemporal completeness, merging these AOD products is then an effective way to produce more spatiotemporally complete and accurate AOD products (Tang et al., 2016). Spatiotemporally complete AOD products would also be expected by the next generation of geostationary satellites as a result of their high temporal resolution (~10 min) that is also possible to adjust hourly $PM_{2.5}$ measurements (Chudnovsky et al., 2012). However, all these passive sensors are not effective in retrievals of aerosols in the presence of clouds. This difficulty could be overcome by introducing lidar observations of aerosol and cloud vertical distributions via active remote sensing, which benefits from rapid developments in emerging networks of automated lidar and space-borne lidar. Automated lidar can not only provide a critical perspective for relating $PM_{2.5}$ to AOD but also identify the specific aerosol types at stations (Baars et al., 2016). The Cloud-Aerosol Lidar with Orthogonal Polarization (CALIOP) has been widely used to improve AOD-$PM_{2.5}$ relationship across the world (Toth et al., 2014). Combination of MODIS with lidar is extremely promising in the $PM_{2.5}$ estimation from AOD. Certainly, Lidar has its limitations that should be kept in mind, for example, limited space coverage, unknown uncertainties in extinction retrievals in the retrieval process and etc. These limitations should be suitably considered in order to optimize the

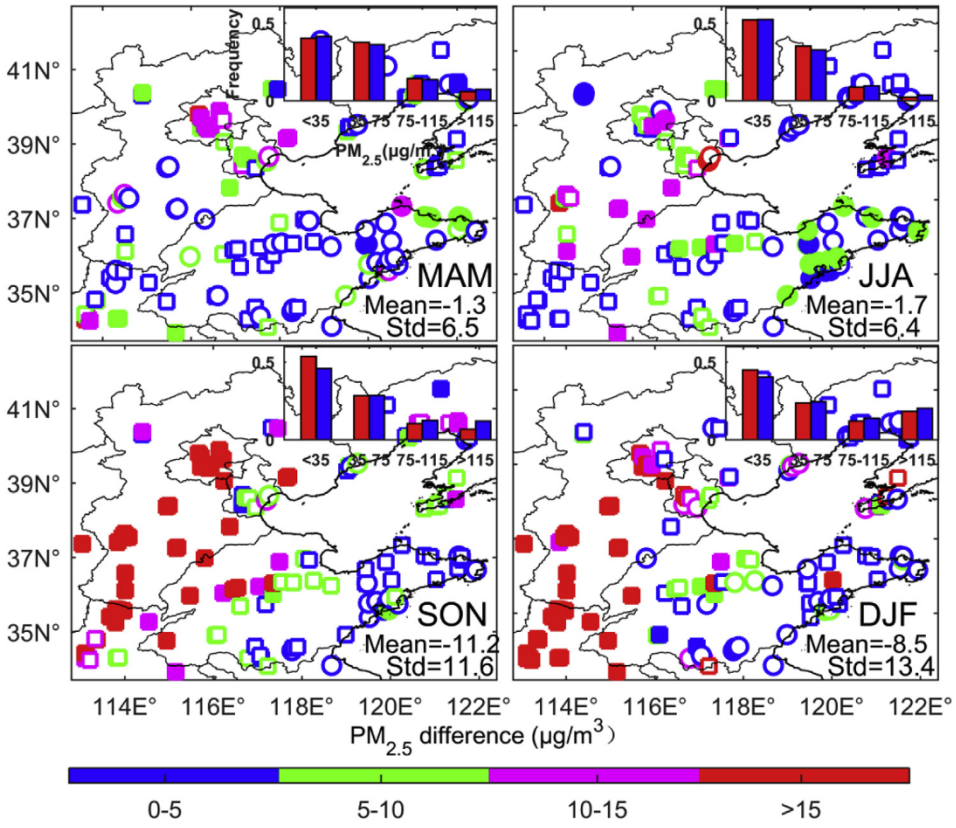

Fig. 8. Seasonal $PM_{2.5}$ differences between $PM_{2.5}$ in the presence and absence of C6.1 AOD. The square and circle represent the difference larger/smaller than zero, respectively. The solid marker means the difference is significant at a confidence level of 95% and the open marker means not. The embedded histogram shows frequency of occurrence of $PM_{2.5}$ values in the presence (red) and absence (blue) of AOD retrievals. (For interpretation of the references to colour in this figure legend, the reader is referred to the Web version of this article.).

strength of Lidar in the estimation of $PM_{2.5}$.

Geo-statistical methods have been developed to fill AOD gaps through incorporation of the temporal and spatial autocorrelation of the AODs alone or both into the synergy, for example, the ordinary Kriging method (Ma et al., 2014), the Bayes Maximum Entropy method (Tang et al., 2016), and the region-specific AOD-$PM_{2.5}$ relationship (KloogKoutrakis et al., 2011, 2014; Lü et al., 2016). AOD relationship to meteorological and land use variables was developed by using the generalized additive mixed model or machine learning algorithm, it was then adopted to fill missing AODs (Liang et al., 2018; Zhang et al., 2018). Synergy of other AOD data sources, for example, AOD products from AERONET or chemical transport models, was also used to enhance AOD availability (Donkelaar et al., 2016; Fu et al., 2018). Note that these techniques differ not only in their data filling efficiencies, but also in their AOD uncertainties. These effects on the $PM_{2.5}$ estimation should be carefully evaluated and comprehensive comparisons between these filling methods are required.

Our results are based on the conventional 10-km MODIS AOD products. A finer resolution AOD is highly required in the air quality study to resolve gradients in $PM_{2.5}$ distribution across urban regions. A new Multi-Angle Implementation of Atmospheric Correction (MAIAC) AOD product with 1-km resolution was released (Lyapustin et al., 2011). Analysis of AOD-$PM_{2.5}$ relationship with varying spatial resolution indicated that the correlation between them decreased significantly as AOD resolution was degraded. AOD sampling rate within 10-km was also enhanced by finer resolution (Chudnovsky et al., 2013a; b; Kloog et al., 2014). Therefore, the MAIAC AOD quality and sampling rate as well as its application to $PM_{2.5}$ estimation in NC needs further study.

Health risk associated with exposure to $PM_{2.5}$ depends on its chemical compositions (Cao et al., 2012), which needs satellite making radiometric, angular and polarimetric measurements. The future satellite missions, for example, Multi-Angle Imager for Aerosols (MAIA), are expected to provide the abundance and characteristics of ground-level aerosol pollution (https://www.jpl.nasa.gov/missions/multi-angle-imager-for-aerosols-maia/).

4. Conclusions

Using 4 years' worth of surface $PM_{2.5}$, AERONET and two versions of Aqua-MODIS AOD data in North China, the accuracy and sampling rate of MODIS AOD products were carefully evaluated, and the potential effect of missing AODs on the estimation of $PM_{2.5}$ was studied. Major conclusions are as follows.

The accuracy of MODIS DT C6.1 AOD in urban areas has been improved. The sampling rates of DT and DB C6.1 AOD products varied slightly relative to that of C6.

The sampling rate of MODIS DT AOD product in winter was on average one order of magnitude smaller than that of the DB product, which would resulted in a biased estimate of $PM_{2.5}$ from this product.

It was suggested to use merged MODIS AOD product in the $PM_{2.5}$ estimation because DT and DB products have similar accuracy and their combination yield the largest sampling rate.

Large bias in $PM_{2.5}$ estimation would be expected if we rely on a subset of days with AOD retrievals to estimate seasonal $PM_{2.5}$ values in fall and winter. The bias in seasonal averages in autumn and winter can exceed 20 $\mu g\, m^{-3}$ in various areas of North China.

Acknowledgements

We greatly appreciate the CMEC archiving and providing hourly $PM_{2.5}$ data. AERONET and MODIS AOD data are downloaded from http://aeronet.gsfc.nasa.gov and https://modis.gsfc.nasa.gov/data/dataprod/mod04.php, respectively. The research is supported by the National Science Foundation of China (91644217 and 41475138) and the National Key R&D Program of China (2016YFC0200403 and 2017YFA0603504). Valuable suggestions of two anonymous reviewers on this paper are greatly appreciated.

Appendix A. Supplementary data

Supplementary data related to this article can be found at https://doi.org/10.1016/j.atmosenv.2019.04.020.

References

Baars, H., Kanitz, T., Engelmann, R., Althausen, D., Heese, B., Komppula, M., Preißler, J., Tesche, M., Ansmann, A., Wandinger, U., Lim, J.-H., Ahn, J.Y., Stachlewska, I.S., Amiridis, V., Marinou, E., Seifert, P., Hofer, J., Skupin, A., Schneider, F., Bohlmann, S., Foth, A., Bley, S., Pfüller, A., Giannakaki, E., Lihavainen, H., Viisanen, Y., Hooda, R.K., Pereira, S.N., Bortoli, D., Wagner, F., Mattis, I., Janicka, L., Markowicz, K.M., Achtert, P., Artaxo, P., Pauliquevis, T., Souza, R.A.F., Sharma, V.P., van Zyl, P.G., Beukes, J.P., Sun, J., Rohwer, E.G., Deng, R., Mamouri, R.-E., Zamorano, F., 2016. An overview of the first decade of PollyNET: an emerging network of automated Raman-polarization lidars for continuous aerosol profiling. Atmos. Chem. Phys. 16, 5111–5137. https://doi.org/10.5194/acp-16-5111-2016.

Cao, J., Xu, H., Xu, Q., Chen, B., Kan, H., 2012. Fine particulate matter constituents and cardiopulmonary mortality in a heavily polluted Chinese city. Environ. Health Perspect. 120, 373–378.

Chudnovsky, A., Lee, H., Kostinski, A., Kotlov, T., Koutrakis, P., 2012. Prediction of daily fine particulate matter concentrations using aerosol optical depth retrievals from the Geostationary Operational Environmental Satellite (GEOS). J. Air Waste Manag. Assoc. 62, 1022–1031.

Chudnovsky, A., Kostinski, A., Lyapustin, A., Koutrakis, P., 2013a. Spatial scales of pollution from variable resolution satellite imaging. Environ. Pol. 172, 131–138.

Chudnovsky, A., Tang, C., Lyapustin, A., Wang, Y., Schewartz, J., Koutrakis, P., 2013b. A critical assessment of high-resolution aerosol optical depth retrievals for fine particulate matter predictions. Atmos. Chem. Phys. 13, 10907–10917.

Cohen, A., Brauer, M., Burnett, R., Anderson, H., Frostad, J., Estep, K., 2017. Estimates and 25-year trends of the global burden of disease attributable to ambient air pollution: an analysis of data from the global burden of diseases study 2015. Lancet 389, 1907–1918.

Donkelaar, A., Martin, R., Brauer, M., Hsu, N., Kahn, R., Levy, R., Lyapustin, A., Sayer, A., Winker, D., 2016. Global estimates of fine particulate matter using a combined geophysical-statistical method with information from satellites, models, and monitors. Environ. Sci. Technol. 50, 3762–3772.

Eck, T.F., Holben, B.N., Reid, J.S., Dubovik, O., Smirnov, A., Neill, N.T.O., Slutsker, I., Kinne, S., 1999. Wavelength dependence of the optical depth of biomass burning,urban , and desert dust aerosols. J. Geophys. Res. 104, 31333–31349.

Eck, T., Holben, B., Reid, J., Xian, P., Giles, D., Sinyuk, A., Smirnov, A., Schafer, J., Slutsker, I., Kim, J., Koo, J., Choi, M., Kim, K., Sano, I., Arola, A., Syer, A., Levy, R., Munchak, L., O'Neill, N., Lyapustin, A., Hsu, N., Randles, C., Silva, A., Buchard, V., Govindaraju, R., Hyer, E., Crawford, J., Wang, P., Xia, X., 2018. Observations of the interaction and transport of fine mode aerosols with cloud and/or fog in Northeast Asia from Aerosol Robotic Network and satellite remote sensing. J. Geophys. Res. 123. https://doi.org/10.1029/2018JD028313.

Engel-Cox, J., Holloman, C., Coutant, B., Hoff, R., 2004. Qualitative and quantitative evaluation of MODIS satellite sensor data for regional and urban scale air quality. Atmos. Environ. 38, 2495–2509.

Fu, D., Xia, X., Wang, J., Zhang, X., Li, X., Liu, J., 2018. Synergy of AERONET and MODIS AOD products in the estimation of PM2.5 concentrations in Beijing. Sci. Rep. 8, 10174. https://doi.org/10.1038/s41598-018-28535-2.

Gupta, P., Christopher, S.A., 2008. An evaluation of Terra-MODIS sampling for monthly and annual particulate matter air quality assessment over the Southeastern United States. Atmos. Environ. 42, 6465–6471.

Gupta, P., Levy, R., Mattoo, S., Remer, L., Munchak, L., 2016. A surface reflectance scheme for retrieving aerosol optical depth over urban surfaces in MODIS dark target retrieval algorithm. Atmos. Meas. Tech. 9, 3293–3308.

Hoff, R., Christopher, S., 2009. Remote sensing of particulate pollution from space: have we reached the promised over land? J. Air Waste Manag. Assoc. 59, 645–675.

Hsu, N., Jeong, M., Bettenhausen, C., Sayer, A., Hansell, R., Seftor, C., Huang, J., Tsay, S., 2013. Enhanced deep blue aerosol retrieval algorithm: the second generation. J. Geophys. Res. 118. https://doi.org/10.1002/jgrd.50712.

Kaufman, Y., Wald, A., Remer, L., Gao, B., Li, R., Flynn, L., 1997. The MODIS 2.1-μm channel-correlation with visible reflectance for use in remote sensing of aerosol. IEEE Trans. Geosci. Remote Sens. 35, 1286–1298.

Kloog, I., Ridgway, B., Koutrakis, P., Coull, B., Schwartz, J., 2013. Long- and short-term exposure to $PM_{2.5}$ and mortality: using novel exposure models. Epidemiology 24, 555–561.

Kloog, I., Chudnovsky, A., Just, A., Nordio, F., Koutrakis, P., Coull, B., Lyapustin, A., Wang, Y., Schwartz, J., 2014. A new hybrid spatio-temporal model for estimating daily multi-year $PM_{2.5}$ concentrations across northeastern USA using high resolution aerosol optical depth data. Atmos. Environ. 95, 581–590.

Kloog, I., Koutrakis, P., Coull, B., Lee, H., Schwartz, J., 2011. Assessing temporally and spatially resolved PM2.5 exposures for epidemiological studies using satellite aerosol optical depth measurements. Atmos. Environ. 45, 6267–6275.

Lee, H., Garay, M., Kalashnikova, V., Yu, Y., Gibson, P., 2018. How long should the MISR record be when evaluating aerosol optical depth climatology in climate models? Rem. Sens. 10, 1326. https://doi.org/10.3390/rs10091326.

Levy, R., Mattoo, S., Munchak, L., Remer, L., Sayer, A., Patadia, F., Hsu, N., 2013. The collection 6 MODIS aerosol products over land and ocean. Atmos. Meas. Tech. 6, 2989–3034.

Li, P., Xin, J., Wang, Y., Wang, S., Li, G., Pan, X., Liu, Z., Wang, L., 2013. The acute effects of fine particles on respiratory mortality and morbidity in Beijing, 2004-2009. Environ. Sci. Pollut. Res. Int. 20, 6433–6444.

Liang, F., Xiao, Q., Wang, Y., Lyapustin, A., Li, G., Gu, D., Pan, X., Liu, Y., 2018. MAIAC-based long-term spatiotemporal trends of $PM_{2.5}$ in Beijing, China. Sci. Total Environ. 616–617, 1589–1598.

Lü, B., Hu, Y., Chang, H., Russell, A., Bai, Y., 2016. Improving the accuracy of daily $PM_{2.5}$ distributions derived from the fusion of ground-level measurements with aerosol optical depth observations, a case study in North China. Environ. Sci. Technol. 50, 4752–4759.

Lyapustin, A., Wang, Y., Laszlo, I., Kahn, R., Korkin, S., Remer, L., Levy, R., Reid, J., 2011. Multi-angle implementation of atmospheric correction (MAIAC): Part 2. Aerosol algorithm. J. Geophys. Res. 116, D03211. https://doi.org/10.1029/2010JD014986.

Ma, Z., Hu, X., Huang, L., Bi, J., Liu, Y., 2014. Estimating ground-level $PM_{2.5}$ in China using satellite remote sensing. Environ. Sci. Technol. 48, 7436–7444.

McGuinn, L., Ward-Caviness, C., Neas, L., Schneider, A., Di, Q., Chudnovsky, A., Schwartz, J., Koutrakis, P., Russell, A., Garcia, V., Kraus, W., Hauser, E., Cascio, W., Sanchez, D., Devlin, R., 2018. Fine particulate matter and cardiovascular disease: comparison of assessment methods for long-term exposure. Environ. Res. 159, 16–23.

Pope, C., Dockery, D., 2006. Health effects of fine particulate air pollution: lines that connect. J. Air Waste Manag. Assoc. 56, 709–742.

Pui, D., Chen, S., Zuo, Z., 2014. $PM_{2.5}$ in China: measurements, sources, visibility and health effects, and mitigation. Particuology 13, 1–26.

Remer, L., Mattoo, S., Levy, R., Munchak, L., 2013. MODIS 3 km aerosol product: algorithm and global perspective. Atmos. Meas. Tech. 6, 1829–1844.

Shi, X., Zhao, C., Jiang, J., Wang, C., Yang, X., Yung, Y., 2017. Spatial representativeness of PM2.5 concentrations obtained using observations from network stations. J. Geophys. Res. 123. https://doi.org/10.1002/2017JD027913.

Song, C., He, J., Wu, L., Jin, T., Chen, X., Li, R., Ren, P., Zhang, L., Mao, H., 2017. Health burden attributable to ambient $PM_{2.5}$ in China. Atmos. Environ. 223, 575–586.

Song, Z., Fu, D., Zhang, X., Wu, Y., Xia, X., He, J., Han, X., Zhang, R., Che, H., 2018. Diurnal and seasonal variability of $PM_{2.5}$ and AOD in North China Plain: comparison of MERRA-2 products and ground measurements. Atmos. Environ. 191, 70–78.

Tang, Q., Bo, Y., Zhu, Y., 2016. Spatiotemporal fusion of multiple-satellite aerosol optical depth (AOD) products using Bayesian maximum entropy method. J. Geophys. Res. 121, 4034–4048.

Tao, M., Chen, L., Wang, Z., Tao, J., Che, H., Wang, X., Wang, Y., 2015. Comparison and evaluation of the MODIS collection 6 aerosol data in China. J. Geophys. Res. 120. http://doi.org/10.1002/2015JDD023360.

Toth, T., Zhang, J., Campbell, J., Hyer, E., Reid, J., Shi, Y., Westphal, D., 2014. Impact of data quality and surface-to-column representativeness on the PM2.5/satellite AOD relationship for the contiguous United States. Atmos. Chem. Phys. 14, 6049–6062.

World Health Organization, 2016. Ambient Air Pollution: a Global Assessment of Exposure and Burden of Disease. https://apps.who.int/iris/bitstream/handle/10665/250141/9789241511353-eng.pdf?sequence=1.

Xia, X., Chen, H., Wang, P., Zhang, W., Goloub, P., Chatenet, B., Eck, T., Holben, B., 2006. Variation of column-integrated aerosol properties in a Chinese urban region. J. Geophys. Res.: Atmos. 111 (D5). https://doi.org/10.1029/2005JD006203.

Xia, X., Zong, X., Sun, L., 2013. Exceptionally active agricultural fire season in mid-eastern China in June 2012 and its impact on the atmospheric environment. J. Geophys. Res. 118. https://doi.org/10.1002/jgrd.50770.

Zha, S., Zhang, S., Cheng, T., Chen, J., Huang, G., Li, X., Wang, Q., 2013. Agricultural fires and their potential impacts on regional air quality over China. Aerosol Air Qual. Res. 13, 992–1001.

Zhang, R., Di, B., Luo, Y., Deng, X., Grieneisen, M., Wang, Z., Yao, G., Zhan, Y., 2018. A nonparametric approach to filling gaps in satellite-retrieved aerosol optical depth for estimating ambient $PM_{2.5}$ level. Environ. Pol. 243, 998–1007.